

Large size LSO and LYSO crystal scintillators for future high-energy physics and nuclear physics experiments

Jianming Chen, Liyuan Zhang, Ren-yuan Zhu*

Lauritsen Laboratory of High Energy Physics, 256-48, California Institute of Technology, Pasadena, CA 91125, USA

Available online 20 November 2006

Abstract

The high energy and nuclear physics community is interested in fast bright heavy crystal scintillators, such as cerium-doped LSO and LYSO. An investigation is being carried out to explore the potential use of the LSO and LYSO crystals in future physics experiments. Optical and scintillation properties, including longitudinal transmittance, emission and excitation spectra, light output, decay kinetics and light response uniformity, were measured for three long ($2.5 \times 2.5 \times 20$ cm) LSO and LYSO samples from different vendors, and were compared to a long BGO sample of the same size. The degradation of optical and scintillation properties under γ -ray irradiations and the radiation-induced phosphorescence were also measured for two long LYSO samples. Possible applications for a crystal calorimeter in future high energy and nuclear physics experiments are discussed.

© 2006 Elsevier B.V. All rights reserved.

PACS: 29.40; 61.80; 81.10; 81.40

Keywords: Lutetium oxyorthosilicate; Lutetium–yttrium oxyorthosilicate; Crystal; Scintillator; Transmission; Emission; Light output; Radiation damage

1. Introduction

Because of their best possible energy resolution, crystal calorimeters have been widely used in high energy and nuclear physics experiments [1]. In the last two decades, cerium-doped silicate-based heavy crystal scintillators have been developed for the medical industry. As of today, mass production capabilities of gadolinium orthosilicate ($\text{Gd}_2\text{SiO}_5\text{:Ce}$ or GSO) [2], lutetium oxyorthosilicate ($\text{Lu}_2\text{SiO}_5\text{:Ce}$ or LSO) [3] and lutetium–yttrium oxyorthosilicate ($\text{Lu}_{2(1-x)}\text{Y}_{2x}\text{SiO}_5\text{:Ce}$, or LYSO) [4,5] are established. These silicates have also attracted an interest in the physics community. The main obstacles of using these crystals in the experimental physics are two-fold: the availability of high-quality crystals in sufficiently large size and the high cost associated with their high melting point (~ 2000 °C). Recent emergence of large size LSO and LYSO crystals, however, inspired this investigation on possible applications of this new generation scintillators in future physics

experiments, such detectors for a super B factory [6] or for the proposed international linear collider [7].

2. Samples and experiment

Fig. 1 is a photo showing four long crystal samples with dimension $2.5 \times 2.5 \times 20$ cm and corresponding cube samples with a dimension of 1.5 rad length (1.7 cm) from four vendors. They are, from top to bottom: BGO samples from Shanghai Institute of Ceramics (SIC), LYSO samples from Crystal Photonics, Inc. (CPI) and Saint-Gobain Ceramics & Plastics, Inc. (Saint-Gobain), and LSO samples from CTI Molecular Imaging, Inc. (CTI). While the SIC and Saint-Gobain long samples have perfect geometry and surface polishing, the CTI long sample is 5 mm shorter, and the CPI long sample has chips at the corners and surfaces since CPI does not have adequate polishing and thermal treatment facilities for such large size samples.

According to manufactures, the yttrium content is about 5% for CPI LYSO [8] and about 10% for Saint-Gobain LYSO [9]. The nominal cerium doping level is 0.2% for CTI LSO [10] and CPI LYSO [8], and is less than 1% for

*Corresponding author. Tel.: +1 626 395 6661; fax: +1 626 795 3951.
E-mail address: zhu@hep.caltech.edu (R.-y. Zhu).

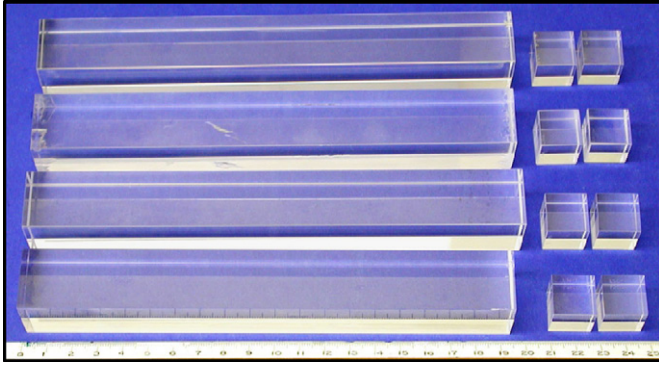


Fig. 1. A photo showing one long ($2.5 \times 2.5 \times 20$ cm) sample and two cubes ($1.7 \times 1.7 \times 1.7$ cm) each from four vendors. From top to bottom: SIC BGO, CPI and Saint-Gobain LYSO and CTI LSO.

Saint-Gobain LYSO [9]. The actual cerium concentration in these crystal samples, however, would be less than the nominal values and its distribution along the long sample's axis also varies because of the segregation. The technical nature of long sample's ends, such as the seed or tail in crystal growth, however, was not provided by manufactures. All surfaces of these samples are polished. No thermal treatment was applied before initial measurements.

The transmittance spectra were measured by using a Hitachi U-3210 UV–visible spectrophotometer with double beam, double monochromator and a large sample compartment with systematic uncertainty of about 0.3%. The excitation, photo-luminescence and radiation-induced phosphorescence spectra were measured using a Hitachi F-4500 fluorescence spectrophotometer. For the excitation and emission spectra, a UV excitation light was shot to a bare surface of the sample, and the crystal was oriented so that its surface normal is at an angle θ with respect to the excitation light. A positive θ indicates that the photo-luminescence is not affected by sample's internal absorption.

The scintillation light output and decay kinetics were measured by using a Photonis XP2254b PMT, which has a multi-alkali photocathode and a quartz window. The sample to be measured was coupled to the PMT with the Dow Corning 200 fluid, while all other faces of the sample were wrapped with the Tyvek paper. A collimated ^{137}Cs source was used to excite cubic samples. Alternatively, a ^{22}Na source was used with coincidence to reduce influence of natural phosphorescence for 20 cm long samples. A Hamamatsu R1306 PMT with high quantum efficiency was used to compare the ^{137}Cs peak energy resolution for these samples.

The uniformity of long samples was evaluated by measuring light outputs at seven evenly distributed positions along crystal's longitudinal axis. The light output responses at these seven points were then fitted to a linear function,

$$\frac{\text{LO}}{\text{LO}_{\text{mid}}} = 1 + \delta \left(\frac{x}{x_{\text{mid}}} - 1 \right) \quad (1)$$

where LO_{mid} represents the light output at the middle of the sample, δ represents the deviation of the light response uniformity and x is the distance from the end coupled to the readout device. Because these samples have a rectangular shape, there are two ways to couple it to the PMT. We define the A end such that the sample produces a lower average light LO_{mid} when it was coupled to the PMT. The other end is defined as the B end.

The degradations of these optical and scintillation properties under γ -ray irradiations were investigated using two irradiation facilities at Caltech: an open 50 Ci ^{60}Co source and a closed 2000 Ci ^{137}Cs source. The former provided dose rates of 2 and 100 rad/h by placing samples at appropriate distances. The later provided dose rates of 9000 rad/h with 5% uniformity when samples were placed at the center of the irradiation chamber. Irradiations were carried out step-by-step with three dose rates of 2, 100 and 9000 rad/h. Each irradiation step lasted for about 1 day. The intensity of radiation-induced phosphorescence in long LYSO samples was also measured as the anode current of a Hamamatsu R2059 PMT with its quartz window coupled to the sample after the third 1-day irradiation under 9000 rad/h.

3. Optical and scintillation properties

3.1. Excitation, emission and transmission spectra

Figs. 2 and 3 show comparison of the transmittance (right scale), emission and excitation spectra (left scale) as a function of wavelength for four cube and long samples, respectively: a SIC BGO, a CTI LSO and two LYSO samples from CPI and Saint-Gobain.

One notes that the LSO and LYSO samples have identical transmittance, excitation and emission spectra. It is also interesting to note that the emission spectra of the LSO and LYSO samples overlap with the absorption edge in their transmittance, while the emission of the BGO sample is well within its transparent wavelength region. This overlap of transmittance and emission spectra, which is much more clearly seen in the long samples as shown in Fig. 3, indicates that the light output of the LSO and LYSO samples is affected by their intrinsic absorption. An improvement of the transmittance in the direction of shorter wavelength would effectively improve the light output for LSO and LYSO crystals. This kind of improvement has been achieved in previous crystal development programs for high-energy physics. One recent example is the development for yttrium-doped lead tungstate crystals for the CMS experiment at LHC [11].

The excitation and emission spectra were also measured at several locations along their longitudinal axis for four long samples. No variations were observed. No variations were observed either in transverse transmittance spectra measured at three locations for four long samples, indicating uniform optical properties along the longitudinal axis of

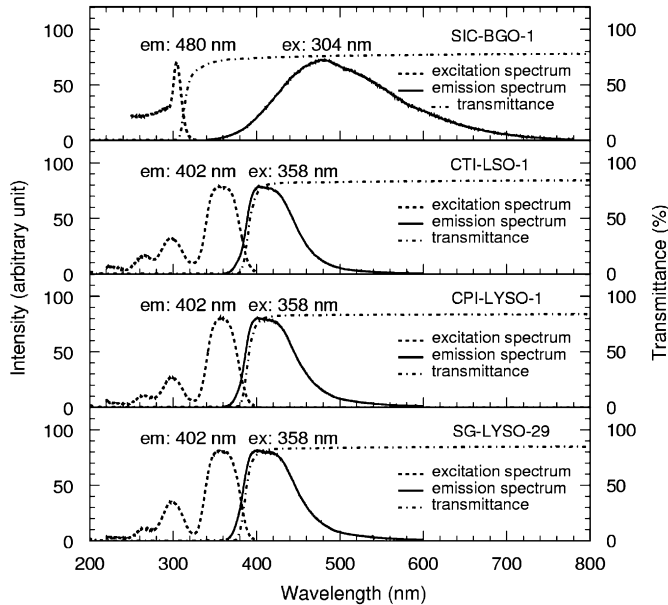


Fig. 2. Optical properties are shown as a function of wavelength for four cube samples. The excitation (dashes) and emission (dots) spectra correspond to the left vertical scale, and the transmittance (solid) spectra to the right.

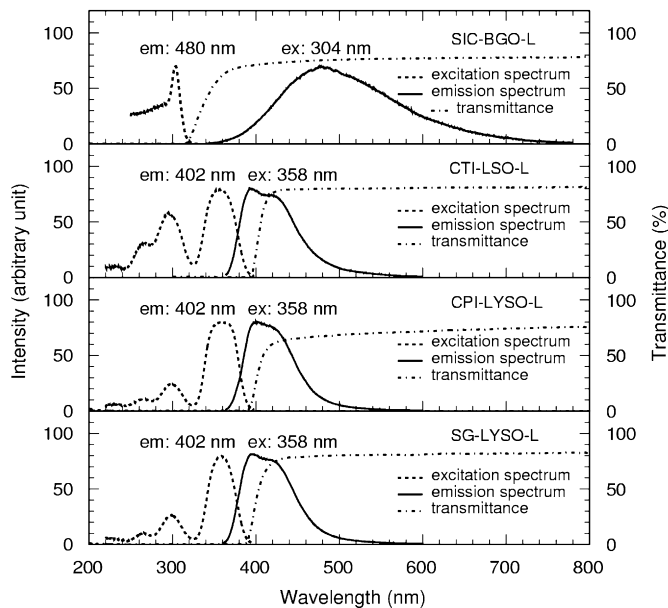


Fig. 3. The same as Fig. 2, for four long samples.

these samples. The transverse transmittance measured for the Saint-Gobain LYSO and CTI LSO samples approaches the theoretical limit [12] calculated by using the refractive index data from Ref. [3]. The longitudinal transmittance of the Saint-Gobain LYSO sample shows an absorption peak at 580 nm, which has no effect on its emission and light output. Poorer transmittance was observed for the CPI

sample, which apparently was caused by its poor surface polishing.

3.2. Light output and decay kinetics

Fig. 4 shows a comparison of self-triggered ^{137}Cs pulse height spectra measured for four cube samples coupled to the R1306 PMT.

The FWHM resolution of the ^{137}Cs peak is 8–9% for LSO and LYSO and 10% for BGO. This resolution is compatible with what obtained by commercially available pixel crystals of much smaller size. Fig. 5 shows a comparison of ^{22}Na (511 keV) pulse height spectra measured with coincidence for four long samples coupled to the R1306 PMT. The FWHM resolution is 10–11% for Saint-Gobain LYSO and CTI LSO, respectively and 15% for SIC BGO. The CPI LYSO sample shows double peak because of inappropriate after growth thermal annealing [8].

Figs. 6 and 7 show comparison of light output and decay kinetics observed for four cube and long samples, respectively coupled to the XP2254b PMT. One notes that the LSO and LYSO samples have consistent decay time and photoelectron yield. While the 300 ns decay time of the BGO sample is a factor of 7 slower as compared to the LSO and LYSO samples, its measured photoelectron yield is a factor of 6 lower. Fig. 8 shows the quantum efficiencies of the R1306 and XP2254b PMT used to measure the pulse height spectra, light output and decay kinetics. Also shown in the figure are the emission spectra for LSO/LYSO and BGO samples as well as the emission-weighted average quantum efficiencies, which can be used to convert the

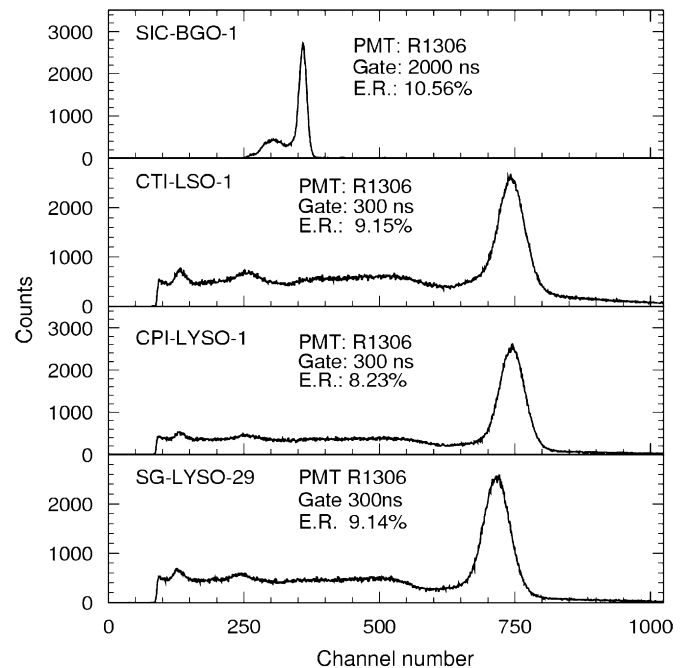


Fig. 4. ^{137}Cs pulse height spectra measured with the R1306 PMT are shown for four cube samples.

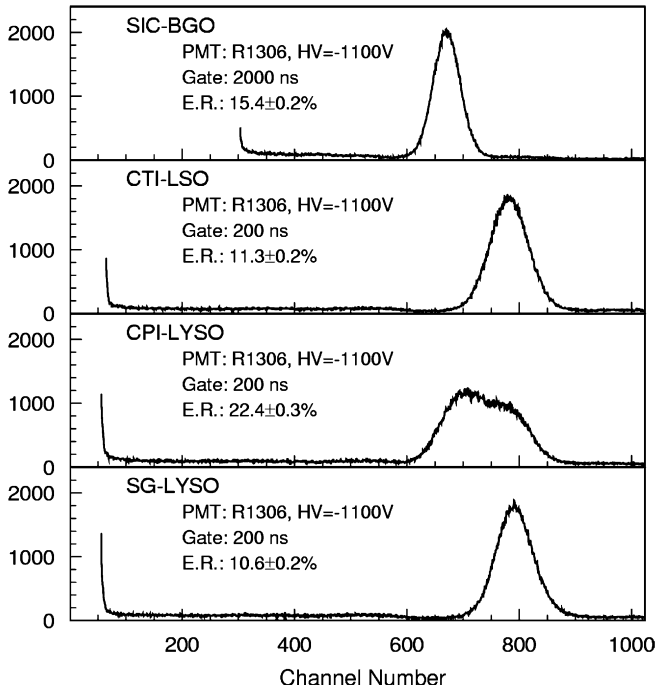


Fig. 5. ^{22}Na pulse height spectra measured with coincidence by the R1306 PMT are shown for four long samples.

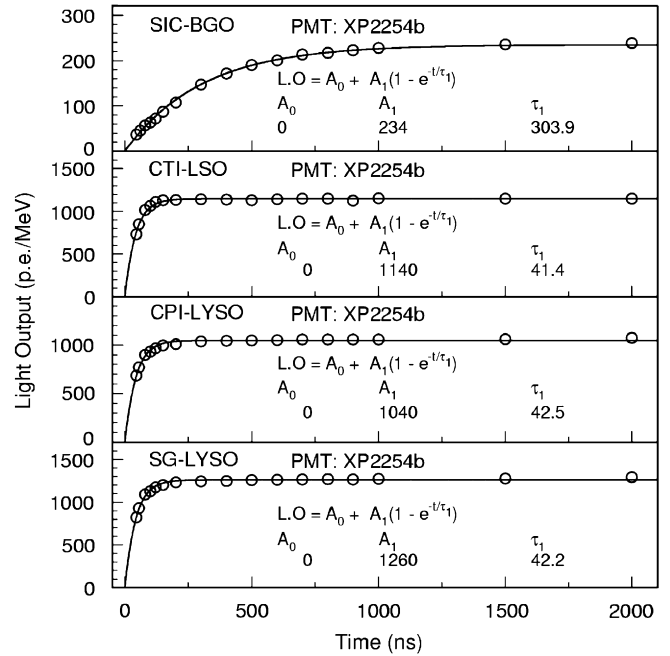


Fig. 7. The same at Fig. 6 for four long samples.

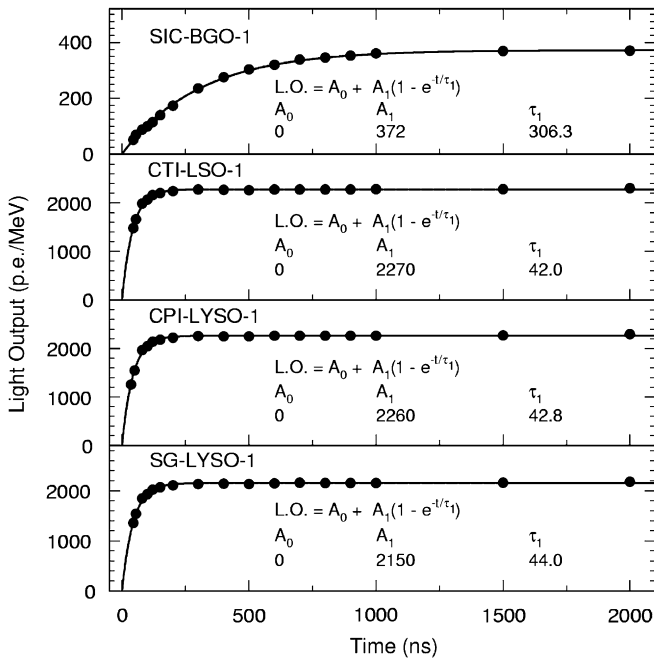


Fig. 6. Light output measured using the XP2254b PMT is shown as a function of the integration time for four cube samples.

measured photoelectron yield to the absolute light output in photon numbers.

Taking into account the PMT response, we conclude that the light yield of LSO and LYSO crystals is a factor of 4 of that of BGO.

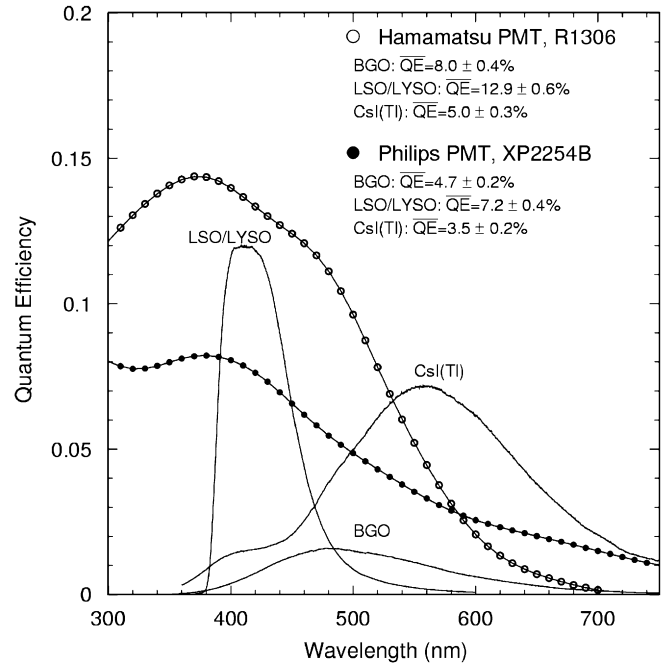


Fig. 8. The quantum efficiencies of the R1306 and XP2254b PMT are shown as a function of wavelength together with the emission spectra of the LSO/LYSO and BGO samples, where the area under the emission curves is roughly proportional to corresponding absolute light output.

3.3. Light response uniformity

Fig. 9 shows the light response uniformity measured using the XP2254b PMT and the corresponding linear fit to Eq. (1) for the Saint-Gobain LYSO sample. Table 1 summarizes the numerical result of the fit. While the BGO

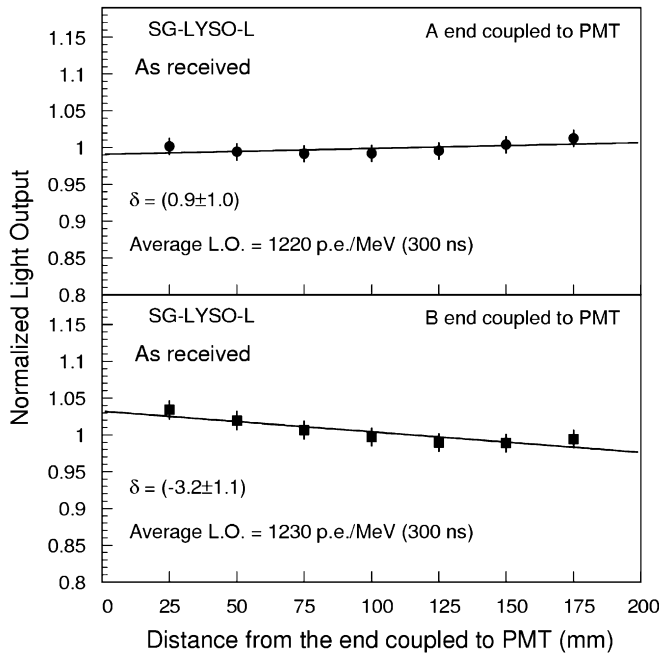


Fig. 9. Light response uniformities are shown with the A (top) and B (bottom) end coupled to the XP2254b PMT for the Saint-Gobain long LYSO sample.

Table 1
Fit result of $LO_{mid} \text{ (p.e./MeV)}/\delta \text{ (\%)}$

Sample	A end coupled	B end coupled
SIC-BGO	232/-1 ± 1	233/-1 ± 1
CTI-LSO	1160/1 ± 1	1160/-9 ± 1
CPI-LYSO	1090/1 ± 1	1120/-3 ± 1
SG-LYSO	1220/1 ± 1	1230/-3 ± 1

sample shows a consistent slight negative δ when both the A and B end coupled to the PMT, long LSO/LYSO samples show different sign of δ when the end coupled to the PMT is switched. This observation hints a slight longitudinal non-uniformity of light yield along the axis in long LSO/LYSO samples. The BGO sample, on the other hand, has a good longitudinal uniformity.

The origin of this difference can be attributed to their chemical nature. While BGO is an intrinsic scintillator, LYSO is a cerium-doped scintillator. It is well known that the light output of these crystals is affected by both the cerium concentration and the yttrium fraction [8,10]. Any longitudinal variation of the cerium concentration and/or the yttrium fraction in LYSO would affect long sample's light response uniformity. To achieve and maintain the excellent energy resolution promised by a crystal calorimeter, effort must be made to develop long crystals of consistent light response uniformity, even under irradiations [1].

4. Radiation damage in long LYSO samples

All known crystal scintillators suffer from radiation damage, which appears in radiation-induced absorption (color centers), reduced scintillation light yield (damage to the scintillation mechanism) and/or radiation-induced phosphorescence (afterglow). While the damage to the absorption or scintillation light yield may lead to a degradation of light output or light response uniformity, the radiation-induced phosphorescence would lead to an increase of the readout noise.

The excitation and emission spectra were measured for two long LYSO samples after the third 1-day irradiation at 9000 rad/h. No variation was observed as compared to that measured before irradiations, indicating no damage in the scintillation mechanism.

Figs. 10 and 11 show expanded views of the longitudinal transmittance spectra measured for two long LYSO samples before and after each 1-day step of γ -ray irradiations at 2, 100 and 9000 rad/h. An immediate increase of 6% and 3% of the emission weighted longitudinal transmittance (EWLT) after the first 1-day irradiation under 2 rad/h was observed for CPI and SG samples, respectively, followed by 6% and 5% degradation under 9000 rad/h. These variation amplitudes, however, are smaller than that of crystal scintillators commonly used in experimental physics [1], indicating that the radiation-induced absorption is a minor effect.

Figs. 12 and 13 compare the light output and the decay kinetics before irradiation and after the third 1-day

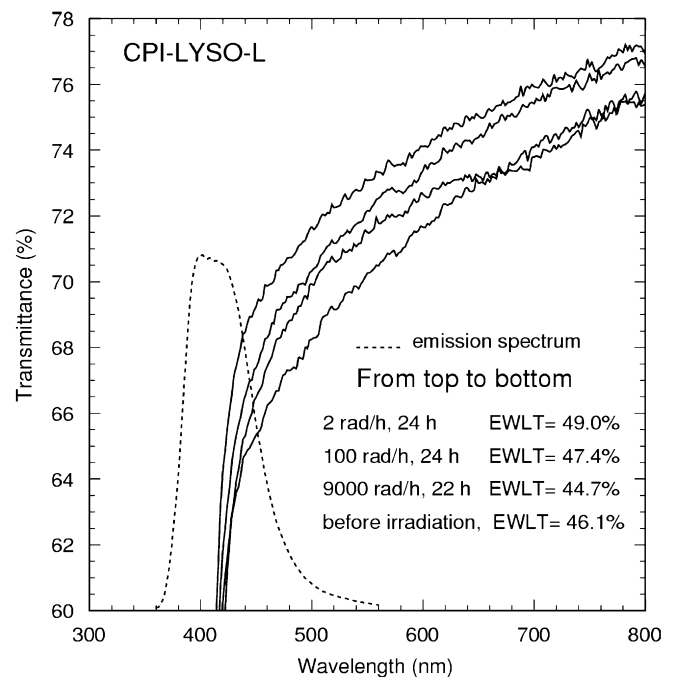


Fig. 10. The longitudinal transmittance spectra (solid curves) before and after 2, 100 and 9000 rad/h irradiations and the emission spectrum (dashes) are shown as a function of wavelength for the CPI long LYSO sample.

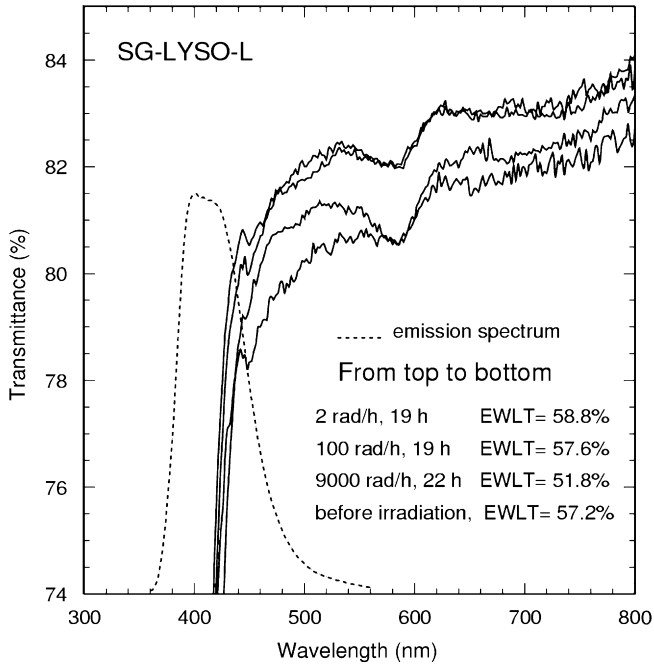


Fig. 11. The same as Fig. 10 for the Saint-Gobain long LYSO sample.

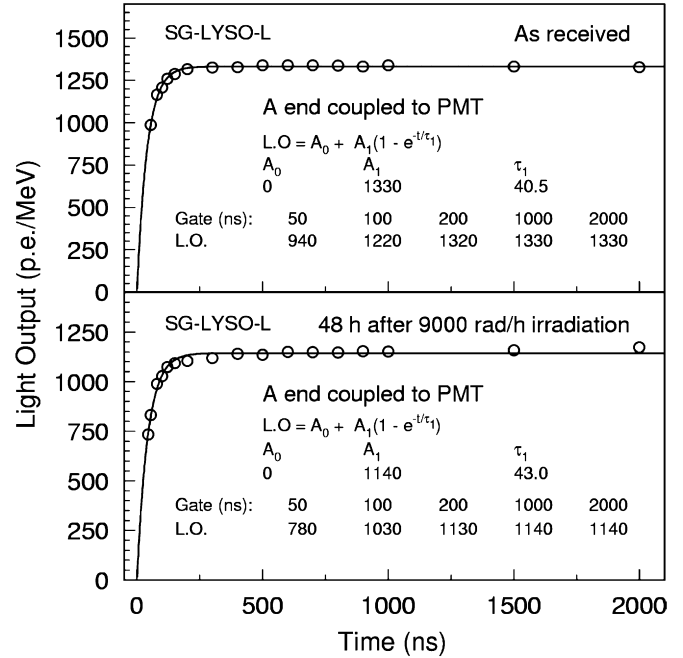


Fig. 13. The same as Fig. 12, for the Saint-Gobain long LYSO sample.

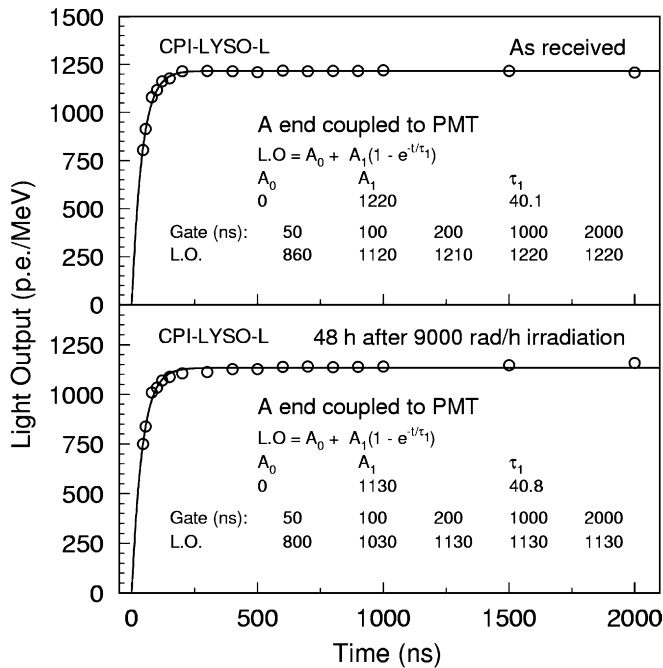


Fig. 12. A comparison of the decay kinetics before and after 22 h irradiation at 9000 rad/h for the CPI long LYSO sample with the A end coupled to the PMT.

irradiation at 9000 rad/h for two long LYSO samples. While some degradation of light output is observed, the decay time remains stable for both samples. Light response uniformities were also measured after the 9000 rad/h irradiation. Comparing to the δ values in Table 1, only

small variations were observed, which is caused by the radiation-induced absorption.

The radiation-induced phosphorescence spectra of the CPI and Saint-Gobain long LYSO samples were measured continuously for more than 48 h after the third 1-day irradiation at 9000 rad/h. No variation of the phosphorescence spectra were observed for both samples. The amplitude of phosphorescence, normalized to 1 h after the end of the irradiation, was fit to an exponential function. The decay time constants of the radiation-induced phosphorescence were determined to be 2.5 and 3.6 h, respectively for the CPI and the Saint-Gobain samples.

To evaluate the consequence of the radiation induced phosphorescence to the readout noise, the Hamamatsu R2059 PMT was used to measure the γ -ray-induced anode current for these LYSO samples under γ -ray-irradiations at 1.2, 3.2 and 14.2 rad/h. Fig. 14 shows the result of this measurement and a linear fit.

Table 2 summarizes the numerical result, where LY is the photoelectron yield of the sample as measured by the R2059 PMT. F is the γ -ray-induced anode current per unit dose rate obtained from the fit. Q_{15} and Q_{500} are the induced photoelectron numbers in 100 ns gate for these two samples under 15 and 500 rad/h, respectively, which were calculated by using the F and the corresponding gain of the R2059 with 900 V bias. σ_{15} and σ_{500} are the corresponding energy equivalent readout noise, which were derived as the r.m.s. fluctuation of the photoelectron numbers. The radiation-induced phosphorescence related readout noise with 100 ns integration time is estimated to be about 0.2 and 1 MeV equivalent under 15 and 500 rad/h, respectively for these two long LYSO samples.

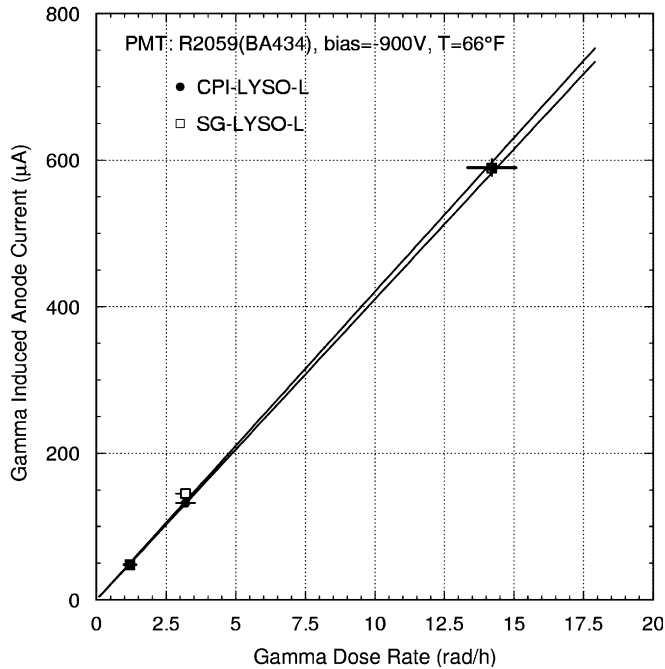


Fig. 14. The γ -ray-induced anode current is shown as a function of the dose rate for the CPI and Saint-Gobain long LYSO samples.

Table 2
 γ -ray-induced readout noise in two long LYSO samples

	CPI LYSO	Saint-Gobain LYSO
LY (p.e./MeV)	1480	1580
F ($\mu\text{A rad}^{-1}\text{h}$)	41	42
Q_{15} (p.e.)	6.98×10^4	7.15×10^4
Q_{500} (p.e.)	2.33×10^6	2.38×10^6
σ_{15} (MeV)	0.18	0.17
σ_{500} (MeV)	1.03	0.97

5. Summary

Ce-doped LSO and LYSO crystals have identical emission, excitation and transmittance spectra. The amplitude of their fast scintillation light with 42 ns decay time is about 4 times of BGO. The absorption edge in their transmittance spectrum affects their light output. One

approach to increase their light output is to improve their absorption edge toward a shorter wavelength. Large size ($2.5 \times 2.5 \times 20$ cm) LSO/LYSO samples from CTI, CPI and Saint-Gobain have good overall longitudinal uniformity in optical and scintillation properties. Their light response uniformity, however, may slightly affect by the distribution of the Ce concentration or the yttrium fraction in the LYSO samples.

Radiation damage on transmittance, emission and light output in LYSO samples is small as compared to other commonly used crystal scintillators. Radiation-induced phosphorescence has a decay time constant of 2.5–3 h. The γ -ray-induced phosphorescence with 100 ns integration time would cause 0.2 and 1 MeV equivalent noise for $2.5 \times 2.5 \times 20$ cm LYSO samples in a radiation environment of 15 or 500 rad/h, respectively.

In a brief summary, with existing mass production capabilities LSO and LYSO crystals are a good candidate for applications in high energy and nuclear physics. Further investigation, however, is needed to understand the performance of these long samples with solid state readout devices, such as Si PD or APD.

Acknowledgments

Useful discussions with Drs. B. Chai, C. Melcher and D. Rothan are acknowledged. This work was supported in part by the US Department of Energy Grant No. DE-FG03-92-ER40701.

References

- [1] R.-Y. Zhu, Nucl. Phys. B 78 (1999) 203.
- [2] K. Takagi, T. Fakazawa, Appl. Phys. Lett. 42 (1983) 43.
- [3] C. Melcher, J. Schweitzer, IEEE Trans. Nucl. Sci. 39 (1992) 502.
- [4] D.W. Cooke, et al., J. Appl. Phys. 88 (2000) 7360.
- [5] T. Kimble, M. Chou, B.H.T. Chai, in: Proceedings of the IEEE Nuclear Science Symposium Conference, 2002.
- [6] W. Wisniewski, R.Y. Zhu (Ed.), in: Proceedings of the Tenth International Conference on Calorimetry in Particle Physics, World Scientific, Singapore, 2002.
- [7] R.-Y. Zhu, talk given at 2005 ILC Workshop, Snowmass, see http://www.hep.caltech.edu/~zhu/talks/ryz_050818_lc.pdf.
- [8] B. Chai, personal communication.
- [9] D. Rothan, private communication.
- [10] C. Melcher, personal communication.
- [11] X. Qu, et al., Nucl. Instr. and Meth. A 480 (2002) 470.
- [12] D. Ma, et al., Nucl. Instr. and Meth. A 333 (1993) 422.